

MeV scale leptonic force for cosmic neutrino spectrum and muon anomalous magnetic moment

Takeshi Araki,^{1,*} Fumihiko Kaneko,¹ Toshihiko Ota,^{1,†} Joe Sato,^{1,‡} and Takashi Shimomura^{2,§}

¹*Department of physics, Saitama University,
Shimo-Okubo 255, 338-8570 Saitama Sakura-ku, Japan*

²*Faculty of Education and Culture, Graduate School of Education, Miyazaki University,
Gakuen-Kibanadai-Nishi 1-1, 889-2192 Miyazaki, Japan*

(Dated: April 14, 2019)

Characteristic patterns of cosmic neutrino spectrum reported by the IceCube collaboration and long-standing inconsistency between theory and experiment in muon anomalous magnetic moment are simultaneously explained by an extra leptonic force mediated by a gauge field with a mass of the MeV scale. With different assumptions for redshift distribution of cosmic neutrino sources, diffuse neutrino flux is calculated with the scattering between cosmic neutrino and cosmic neutrino background through the new leptonic force. Our analysis sheds light on a relation among lepton physics at the three different scales, PeV, MeV, and eV, and provides possible clues to the distribution of sources of cosmic neutrino and also to neutrino mass spectrum.

PACS numbers: 13.15.+g, 14.60.Ef, 95.55.Vj, 98.70.Sa,

Keywords: Neutrino interactions, Cosmic neutrinos, IceCube, Muon anomalous magnetic moment,

I. INTRODUCTION

Astrophysics and also neutrino physics enter a new era after the discovery of high energy cosmic neutrino events observed by the IceCube collaboration [1, 2]. The follow-up reports [3–6] with additional statistics uncover the spectrum of cosmic neutrino in the energy range between $\mathcal{O}(10)$ TeV and $\mathcal{O}(1)$ PeV. The reported spectrum shows some remarkable features, for example, (i) The neutrino flux diminishes steeply as the energy increases, and the best-fit spectral index is $s_\nu = 2.5$ [6], (ii) There is a gap in the energy range between 400 TeV and 1 PeV [3, 6]. The high spectral index is consequent on the sudden end of the spectrum at the high energy edge ($E_\nu \simeq 3$ PeV) and high event rate at the low energy bin $E_\nu \lesssim 100$ TeV [4–8]. In contrast, in Refs. [9–11], it is also pointed out that neutrino spectrum with the spectral index higher than $s_\nu \gtrsim 2.2$ causes a serious conflict with the gamma-ray observation at Fermi-LAT, if the spectrum does not have cut-off at the low energy. The presence of the gap may also urge reconsideration of the assumption of simple power-law spectrum which is typically resulted from standard hadronuclear process (pp inelastic scattering) in the so-called cosmic-ray reservoir such as galaxy cluster. Although any of these features in the spectrum have not been conclusive in statistics, plenty of attempts have been made to reproduce them from the aspects of both astrophysics [10–15] (for a review, see Ref. [16]) and particle physics [17–48].

In Refs. [39–46], the origin of the gap in the observed spectrum was asked to the attenuation of cosmic neu-

trino, which is caused by the scattering with cosmic neutrino background (CνB) through a new interaction between neutrinos, the so-called neutrino secret interaction [49].¹ In such a scenario, the narrow width of the gap can be explained by the resonant behaviour of the scattering. In the previous study [43], we introduced a new gauged leptonic force to explain the gap and pointed out that the leptonic force could simultaneously explain the disagreement between theory and experiment in muon anomalous magnetic moment. We improve in this paper our numerical method and calculate diffuse neutrino flux, taking account of the distribution of the source of cosmic neutrino with respect to the redshift. Moreover, we search through the model parameter space to find a set of parameters that can reproduce not only the gap but also the sharp edge at the upper end of the cosmic neutrino spectrum. The existence of the edge is expected to improve the fit of spectrum with a lower value of spectral index to the observation. Here we also discuss constraints to the model, some of which were not considered in our previous study, such as the neutrino-electron scattering process, invisible decay of a light particle at colliders, big bang nucleosynthesis, and supernova neutrino.

The paper is organized as follows: In the second section, we will describe our model and illustrate parameter regions relevant to cosmic neutrino spectrum and muon anomalous magnetic moment. We will also discuss constraints from laboratory experiments and cosmological and astrophysical observations. Differential equations for diffuse neutrino flux with the leptonic force will be given in Sec. III. The spectra calculated with different model parameters and redshift distribution of cosmic neutrino sources will be compared with the observation in Sec. IV.

* araki@krishna.th.phy.saitama-u.ac.jp

† toshi@mail.saitama-u.ac.jp

‡ joe@phy.saitama-u.ac.jp

§ shimomura@cc.miyazaki-u.ac.jp

¹ The effect on the cosmic neutrino spectrum from the scattering between neutrino and dark matter is discussed in Refs. [44, 50].

Finally, we will discuss the relation between the characteristic features of cosmic neutrino spectrum and neutrino mass spectrum, and also distribution of sources of cosmic neutrino.

II. MODEL AND CONSTRAINTS

We extend the standard model (SM) of particle physics with a massive vector boson Z' that mediates a new leptonic force,

$$\mathcal{L}_{\text{int}} = g_{Z'} Q_{\alpha\beta} [\bar{L}_\alpha \gamma^\rho L_\beta + \bar{\ell}_{R\alpha} \gamma^\rho \ell_{R\beta}] Z'_\rho, \quad (1)$$

where L_α and $\ell_{R\alpha}$ are a lepton doublet and a right-handed charged lepton singlet with flavour $\alpha = \{e, \mu, \tau\}$ respectively. We choose the flavour structure of the interaction as $Q_{\alpha\beta} = \text{diag}(0, 1, -1)$ which corresponds to the $U(1)$ gauge interaction associated with muon number minus tau number ($L_\mu - L_\tau$) [51, 52]. In this paper, we do not discuss the details of the model, such as a mechanism of the symmetry breaking². Instead, we handle the two parameters, the coupling $g_{Z'}$ and the mass $M_{Z'}$ of the gauge boson, as parameters that describe the model.

The interaction with neutrinos in Eq. (1) is expected to produce the gap and the edge in the cosmic neutrino spectrum through the resonant scattering with $C\nu B$. In the resonant scattering process $\nu_{\text{Cosmic}} \bar{\nu}_{C\nu B} \rightarrow \nu \bar{\nu}$ mediated by Z' , only cosmic neutrinos having the energy corresponding to the resonance energy E_{res} are selectively scattered off by $C\nu B$ on the way from its source to the IceCube [39–43, 45, 46], which results in the gap around E_{res} . Here, E_{res} is given as

$$E_{\text{res}} = \frac{M_{Z'}^2}{2m_\nu(1+z)} \quad (2)$$

where m_ν stands for a mass of the target $C\nu B$ and z is the redshift parameter at which the scattering occurs. In Eq. (2), the $C\nu B$ is assumed to be at rest. With an assumption of $m_\nu = \mathcal{O}(0.1)$ eV, the scale of $M_{Z'}$ can be estimated as $M_{Z'} = \mathcal{O}(1 - 10)$ MeV for $E_{\text{res}} \simeq 1$ PeV. Meanwhile, in order to sufficiently scatter cosmic neutrino during the travel of $\mathcal{O}(1)$ Gpc, the size of the cross section is required to be larger than $\sim 10^{-30}$ cm² at the resonance [39, 40]. In the $L_\mu - L_\tau$ model, the cross section near the resonance is estimated as³

$$\sigma_{\text{res}} = \frac{2\pi g_{Z'}^2}{M_{Z'}^2} \delta\left(1 - \frac{M_{Z'}^2}{s}\right), \quad (3)$$

² Although we do not fully describe the model Lagrangian, we assume that the Yukawa sector also respects the symmetry, and it is broken so as not to shift the mass eigenbasis of charged leptons, i.e., the lepton flavour is not violated. The gauge symmetry and its phenomenology have been discussed in Refs. [53–62].

³ In the numerical calculation, the scattering cross section in the neutrino mass eigenbasis is used, cf. Eqs. (7) and (8).

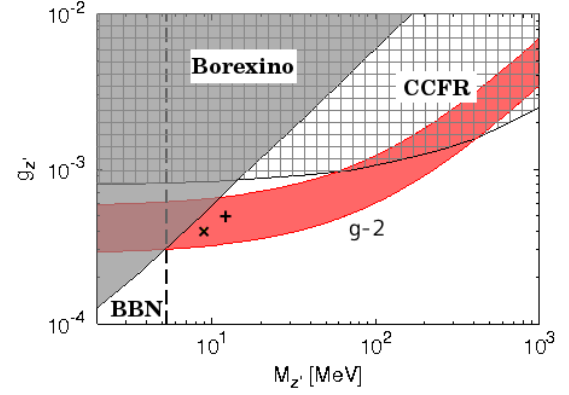


FIG. 1. Relevant parameter region and the constraints. The red band represents a parameter region favoured by muon anomalous magnetic moment within 2σ . The hatched region is excluded by the lepton trident search at the CCFR experiment. The region excluded by the measurement of $\nu e \rightarrow \nu e$ at Borexino is filled with a gray colour. The vertical dashed line stands for the lower bound on $M_{Z'}$ from BBN. Two symbols + and \times indicate $(M_{Z'}, g_{Z'}) = (11 \text{ MeV}, 5 \times 10^{-4})$ and $(9 \text{ MeV}, 4 \times 10^{-4})$, respectively, which are used in Sec. IV. See text for details.

where $s = 2m_\nu E_\nu$ is the square of the center-of-mass energy. The requirement to the cross section turns out to be $g_{Z'} \gtrsim \mathcal{O}(10^{-4})$. Putting it all together, the model parameter region that is relevant to the cosmic neutrino spectrum at the energy range around 1 PeV can be deduced as

$$g_{Z'} \gtrsim \mathcal{O}(10^{-4}) \text{ and } M_{Z'} = \mathcal{O}(1 \sim 10) \text{ MeV}. \quad (4)$$

The interaction with charged leptons (namely muons) in Eq. (1) is responsible to an extra contribution to muon anomalous magnetic moment. The measurement [63] is deviated from the SM predictions [64–67] by around 3σ . The extra contributions from various types of new physics to fill this discrepancy have been intensively studied [68] and also in the context of the $L_\mu - L_\tau$ model [69]. The Z' contribution with the combinations of $g_{Z'}$ and $M_{Z'}$ indicated with the red band in Fig. 1 successfully reproduces the observed value of muon anomalous magnetic moment within 2σ errors. In Fig. 1, we also show some experimental constraints (see below) on the model, which pin down the model parameter region onto

$$g_{Z'} \sim \mathcal{O}(10^{-4}) \text{ at } M_{Z'} = \mathcal{O}(10) \text{ MeV}. \quad (5)$$

It is worth noting that this parameter region has some overlap with the region Eq. (4) required to reproduce the gap and the edge in the cosmic neutrino spectrum.

In the following, we summarize experimental constraints on the $L_\mu - L_\tau$ model.

◦ **Neutrino trident production process:** In the mass region ($M_{Z'} \lesssim 100$ MeV) we are working with, the tightest constraint comes from searches for the neutrino trident process: the production process of a $\mu^- \mu^+$ pair with a muon-neutrino, which is resulted from the scattering of

a muon neutrino from a target nucleus. The process was observed at several neutrino beam experiments, e.g., the CHARM-II [70] and the CCFR [71]. Since the reported results are in good agreement with the SM prediction, which is mediated by the Z and the W bosons, an additional contribution to the process mediated by Z' , whose amplitude is proportional to $g_{Z'}^2$, is strongly constrained. Indeed, the constraint on $M_{Z'}$ and $g_{Z'}$ was recently evaluated in Ref. [72]. We adopt the 95% C.L. bound of the CCFR experiment, which is shown in Fig. 1 as a hatched region.

◦ **Neutrino-electron scattering:** Although electron is not charged under the $L_\mu - L_\tau$ symmetry, Z' can interact with electron through a kinetic mixing ϵ between Z' and photon, which is induced by loop diagrams. The total contribution to the kinetic mixing ϵ in the $L_\mu - L_\tau$ model is finite, and it is estimated as

$$|\epsilon_{\text{loop}}| = \frac{8}{3} \frac{eg_{Z'}}{(4\pi)^2} \ln \frac{m_\tau}{m_\mu} = 7.2 \cdot 10^{-6} \left(\frac{g_{Z'}}{5 \cdot 10^{-4}} \right), \quad (6)$$

where e is the elementary electric charge. This leads an extra contribution to the elastic $\nu e \rightarrow \nu e$ scattering signal in the solar neutrino measurement at the Borexino experiment. The amplitude is proportional to $\epsilon eg_{Z'}/(q^2 - M_{Z'}^2)$, where q^2 is the momentum transfer. The constraints from Borexino are discussed in Refs. [73–75] in the context of various different scenarios of new leptonic force. We here interpret the bounds given in Ref. [73] to that in the $L_\mu - L_\tau$ model while taking account of the fraction of mass eigenstates of solar neutrino, which is given in Ref. [76]. In Fig. 1, the excluded region is filled with a gray colour. The measurement of ν - e elastic scattering at LSND [77] places a similar bound to the coupling $g_{Z'}$ at $M_{Z'} \simeq 10$ MeV (and a weaker bound at $M_{Z'} \simeq 1$ MeV) [75].

◦ **Beam dump experiments:** Once the kinetic mixing between photon and Z' appears, Z' can be produced on shell at beam dump experiments, whose production rate is $\mathcal{O}(e^2 e^2)$. However, the Z' immediately decays into the neutrino-anti-neutrino channel in the $L_\mu - L_\tau$ model. Therefore, the constraints from the search for e^+e^- pairs at the detectors located downstream of the beam dump, such as E137 [78, 79], are irrelevant for our scenario.

◦ **Invisible decay of a light particle:** Since Z' in this framework decays dominantly to $\nu\bar{\nu}$, one of the smoking-gun signals in collider experiments is a light particle decaying to an invisible mode. The kinetic mixing leads the on-shell production of Z' . The process, $e^+e^- \rightarrow \gamma Z' \rightarrow \gamma + \text{invisible}$, is searched at BaBar [80], which sets the bound to the coupling between electron and Z' at $\sim 10^{-3}$ [81]. Our reference choices of parameters satisfy this condition.

◦ **Big Bang Nucleosynthesis (BBN):** A constraint on $M_{Z'}$ is derived from BBN. If Z' is as light as the temperature at the era of BBN, its existence increases the number of relativistic degrees of freedom, N_{eff} , and

the success of the standard BBN might be spoiled, which leads the lower bound $M_{Z'} \gtrsim 1$ MeV [82]. This condition is always satisfied on the parameter region of our interest. Nevertheless, Z' with a mass of $\mathcal{O}(10)$ MeV may indirectly contribute to N_{eff} through a raise in the temperature of ν_μ and ν_τ [45]. In Fig. 1, we display the lower bound on $M_{Z'}$ from the indirect contribution with $\Delta N_{\text{eff}} < 0.7$ as a vertical dashed line, which is taken from Ref. [45].

◦ **Other constraints and future improvement:**

There exist many other experimental observations constraining the $L_\mu - L_\tau$ model. Most of them, however, are either irrelevant in the mass region we are focusing on (i.e. $M_{Z'} < 100$ MeV) or weaker than the bounds discussed above. We here mention some of them; Searches for the SM Z boson decay to four leptons at the LHC can be used to constrain the $L_\mu - L_\tau$ model [57, 58]. However, it becomes insensitive in the mass region below $M_{Z'} \simeq 10$ GeV [72] due to the invariant mass cut for the same-flavour leptons. Furthermore, Z' alters the decay rates of Z , W , and mesons, but constraints from them are weaker than the CCFR bound [83, 84]. The bound from a precise measurement of cosmic microwave background anisotropy is much weaker than those discussed above, cf. Fig. 1 in [40] and discussion in Refs. [85, 86].

It should be noted that a severe constraint on $g_{Z'}$ possibly arises from supernova neutrino observations [45]. The existence of Z' with an MeV-scale mass interrupts free-streaming of ν_μ and ν_τ in the core, which could make the diffusion time much longer than the estimation from the standard supernova cooling process. To avoid the possible problem, an introduction of an additional invisible particle, e.g. the QCD axion, might be necessary.

Apart from astrophysical/cosmological observations and the constraints through the kinetic mixing term, a direct test of a muonic force mediated by a boson with a sub-GeV mass is planned at CERN SPS [87], which is expected to improve the sensitivity to the coupling $g_{Z'}$ by orders of magnitude and fully cover the parameter region referred at Eqs. (4) and (5). We expect that the trident events have been recorded at near detectors in modern long-baseline neutrino oscillation experiments, which may be accessible in the present moment. This might already give us an opportunity to explore the relevant parameter region.

III. DIFFUSE NEUTRINO FLUX

In order to calculate diffuse neutrino flux ϕ_{ν_i} observed at IceCube, we numerically solve the simultaneous partial differential equations with respect to differential number density $\tilde{n}_{\nu_i}(E_{\nu_i}, z)$ of cosmic neutrino ν_i , which are given in Refs. [40, 46]:

$$\frac{\partial \tilde{n}_{\nu_i}}{\partial t} = \frac{\partial}{\partial E_{\nu_i}} b \tilde{n}_{\nu_i} + \mathcal{L}_{\nu_i} - c n_{\text{CMB}} \tilde{n}_{\nu_i} \sum_j \sigma(\nu_i \bar{\nu}_j^{\text{CMB}} \rightarrow \nu \bar{\nu})$$

$$\begin{aligned}
& + cn_{C\nu B} \sum_{j,k} \int_{E_{\nu_i}}^{\infty} dE_{\nu_k} \tilde{n}_{\nu_k} \frac{d\sigma(\nu_k \bar{\nu}_j^{C\nu B} \rightarrow \nu_i \bar{\nu})}{dE_{\nu_i}} \\
& + cn_{C\nu B} \sum_{j,k} \int_{E_{\nu_i}}^{\infty} dE_{\bar{\nu}_k} \tilde{n}_{\bar{\nu}_k} \frac{d\sigma(\bar{\nu}_k \nu_j^{C\nu B} \rightarrow \nu_i \bar{\nu})}{dE_{\nu_i}},
\end{aligned} \tag{7}$$

$$\begin{aligned}
\frac{\partial \tilde{n}_{\bar{\nu}_i}}{\partial t} = & \frac{\partial}{\partial E_{\bar{\nu}_i}} b \tilde{n}_{\bar{\nu}_i} + \mathcal{L}_{\bar{\nu}_i} - cn_{C\nu B} \tilde{n}_{\bar{\nu}_i} \sum_j \sigma(\bar{\nu}_i \nu_j^{C\nu B} \rightarrow \nu \bar{\nu}) \\
& + cn_{C\nu B} \sum_{j,k} \int_{E_{\bar{\nu}_i}}^{\infty} dE_{\bar{\nu}_k} \tilde{n}_{\bar{\nu}_k} \frac{d\sigma(\bar{\nu}_k \nu_j^{C\nu B} \rightarrow \bar{\nu}_i \nu)}{dE_{\bar{\nu}_i}} \\
& + cn_{C\nu B} \sum_{j,k} \int_{E_{\bar{\nu}_i}}^{\infty} dE_{\nu_k} \tilde{n}_{\nu_k} \frac{d\sigma(\nu_k \bar{\nu}_j^{C\nu B} \rightarrow \bar{\nu}_i \nu)}{dE_{\bar{\nu}_i}},
\end{aligned} \tag{8}$$

where $i, j, k = \{1, 2, 3\}$ are the indices for neutrino mass eigenstates. The time t is related to redshift z as $\frac{dz}{dt} = -(1+z)H(z)$. Following the discussion in Ref. [88], we treat cosmic neutrino as incoherent sum of mass eigenstates. The first term in the right-hand-side is responsible to energy loss of cosmic neutrino, owing to redshift, and the energy-loss rate b is given with $b = H(z)E_{\nu}$. The second term represents the influx from sources of cosmic neutrino. In this study, we assume that all sources provide the same spectrum of cosmic neutrino, i.e., $\mathcal{L}_{\nu_i}(E_{\nu_i}, z)$ is simply parametrized as $\mathcal{L}_{\nu_i}(E_{\nu_i}, z) = \mathcal{W}(z)\mathcal{L}_0(E_{\nu_i})$ with the cosmic neutrino spectrum $\mathcal{L}_0(E_{\nu})$ from each source and the source distribution $W(z)$ with respect to redshift z . Here, source distribution function is assumed to be common for all the mass eigenstates of cosmic neutrino. We adopt a power-law spectrum, which is characterised with the spectral index s_{ν} and the cut-off energy E_{cut} :

$$\mathcal{L}_0(E_{\nu}) = \mathcal{Q}_0 E_{\nu}^{-s_{\nu}} \exp\left[-\frac{E_{\nu}}{E_{\text{cut}}}\right], \tag{9}$$

where \mathcal{Q}_0 is the normalization of the flux, which will be adjusted so as to fit to the observed flux. This type of spectrum is typically resulted from hadronuclear process (pp inelastic scattering) in cosmic-ray reservoir, and the values of s_{ν} and E_{cut} are expected to be determined by properties (acceleration rate, i.e., magnetic field and size [89]) of cosmic neutrino source. The flavour composition of cosmic neutrino from pp reaction is expected to be $(\nu_e, \nu_{\mu}, \nu_{\tau}; \bar{\nu}_e, \bar{\nu}_{\mu}, \bar{\nu}_{\tau}) = (1, 2, 0; 1, 2, 0)$ at each source, which leads that each mass eigenstate is produced approximately with an equal rate, i.e., the normalization factor \mathcal{Q}_0 is assumed to be common to all the mass eigenstates in our calculations. Although the sources of the PeV cosmic neutrinos have not been identified yet, we assume the following function inspired from the star formation rate (SFR) [90] as a test distribution:

$$\mathcal{W}(z) = \begin{cases} (1+z)^{3.4} & 0 \leq z < 1, \\ (1+z)^{-0.3} & 1 \leq z \leq 4. \end{cases} \tag{10}$$

The third term represents the outflows caused by the scattering process with $C\nu B$. Here, the cross section σ is

$$\sigma(\nu_i \bar{\nu}_j^{C\nu B} \rightarrow \nu \bar{\nu}) = \frac{|g'_{ji}|^2 g_{Z'}^2}{6\pi} \frac{s}{(s - M_{Z'}^2)^2 + M_{Z'}^2 \Gamma_{Z'}^2}, \tag{11}$$

where $\Gamma_{Z'} = g_{Z'}^2 M_{Z'}/(12\pi)$ is the total decay width of Z' . The coupling $g'_{ij} = g_{Z'}(U^\dagger)_{i\alpha} Q_{\alpha\beta} U_{\beta j}$ is the coupling in the mass eigenbasis, where U is the lepton mixing matrix. The number density of cosmic neutrino background is given as $n_{C\nu B} = 56(1+z)^3/\text{cm}^3$ for each degree of freedom. The constant c appears in the third, forth, and fifth terms is the light speed. The forth and the fifth terms provide the influx from the final states of the scattering process, the so-called regeneration terms. The differential cross sections for cosmic neutrino ν_i are calculated to be

$$\begin{aligned}
\frac{d\sigma(\nu_k \bar{\nu}_j^{C\nu B} \rightarrow \nu_i \bar{\nu})}{dE_{\nu_i}} = & \frac{|g'_{jk}|^2 \sum_l |g'_{il}|^2 m_{\nu_j} E_{\nu_i}^2}{2\pi E_{\nu_k}^2} \\
& \times \frac{1}{(s - M_{Z'}^2)^2 + M_{Z'}^2 \Gamma_{Z'}^2},
\end{aligned} \tag{12}$$

$$\begin{aligned}
\frac{d\sigma(\bar{\nu}_k \nu_j^{C\nu B} \rightarrow \nu_i \bar{\nu})}{dE_{\nu_i}} = & \frac{|g'_{kj}|^2 \sum_l |g'_{il}|^2 m_{\nu_j} (E_{\nu_k} - E_{\nu_i})^2}{2\pi E_{\nu_k}^2} \\
& \times \frac{1}{(s - M_{Z'}^2)^2 + M_{Z'}^2 \Gamma_{Z'}^2}.
\end{aligned} \tag{13}$$

For cosmic anti-neutrino $\bar{\nu}_i$, the differential cross section for the scattering process $\bar{\nu}_k \nu_j^{C\nu B} \rightarrow \bar{\nu}_i \nu$ ($\nu_k \bar{\nu}_j^{C\nu B} \rightarrow \bar{\nu}_i \nu$) is the same as Eq. (12) (Eq. (13)). We numerically solve these simultaneous partial differential equations Eqs. (7) and (8) of cosmic neutrino propagation, following the algorithms introduced in Ref. [91]. We confirmed that our numerical method correctly reproduces the results given in Ref. [40]. After the simultaneous equations are solved, the differential number density \tilde{n}_{ν_i} of cosmic neutrino at the Earth ($z = 0$) is obtained, and the neutrino flux ϕ_{ν_i} observed at IceCube is calculated as

$$\phi_{\nu_i}(E_{\nu_i}) = \frac{c}{4\pi} \tilde{n}_{\nu_i}(E_{\nu_i}, z = 0). \tag{14}$$

In the next section, we will plot the total fluxes $\Phi = \sum_i (\phi_{\nu_i} + \phi_{\bar{\nu}_i})$ as functions of the observed energy of cosmic neutrinos.

IV. NUMERICAL RESULTS

We numerically solve the Eqs. (7) and (8) and calculate the cosmic neutrino flux in the presence of the $L_{\mu} - L_{\tau}$ interaction. Throughout the numerical study, we do not take account of the effect of thermal distribution of the $C\nu B$ momentum. This treatment is justified by our choices of the parameters; We are mainly interested in the parameter region where the lightest neutrino mass is much larger than the $C\nu B$ temperature, cf. Fig. 2.

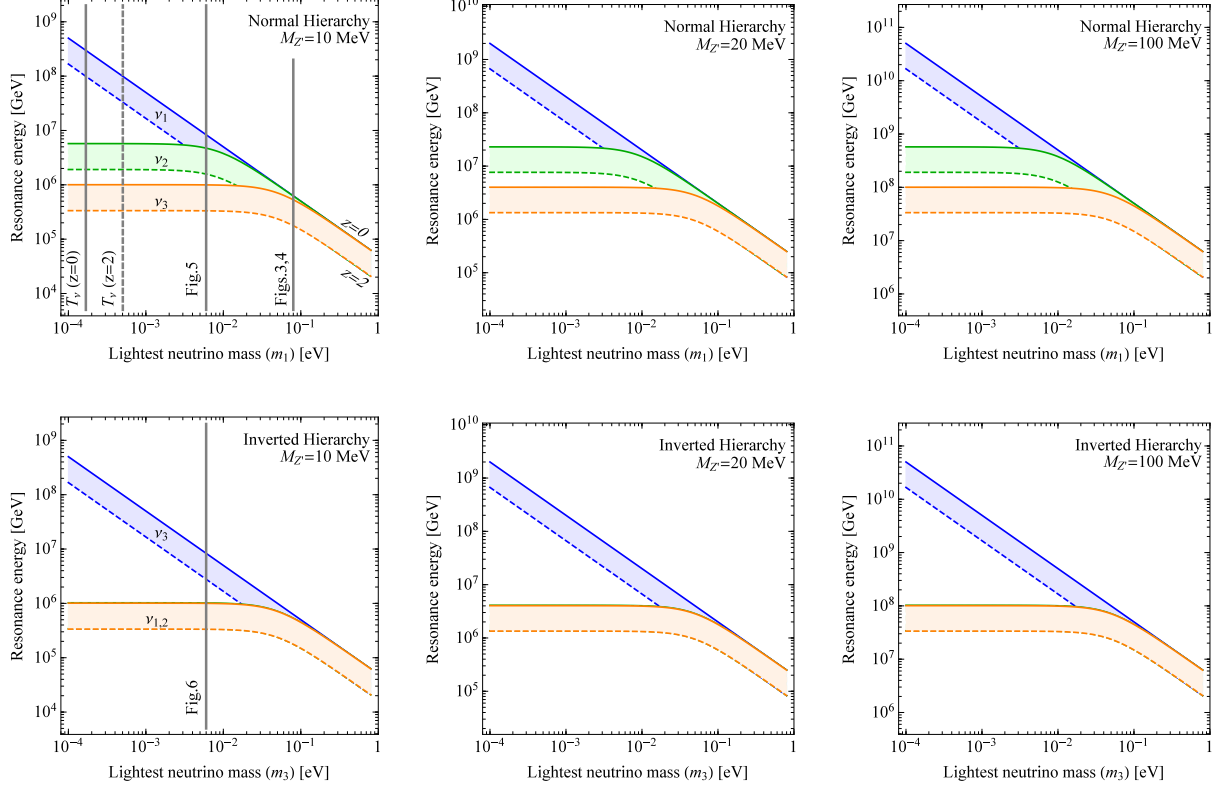


FIG. 2. Resonance energies as functions of the lightest neutrino mass. The mass $M_{Z'}$ of the leptonic gauge boson is taken to be $\{10, 20, 100\}$ MeV, and the redshift z of the scattering point is varied between $z = 0$ (solid) and $z = 2$ (dashed). The band labelled with “ ν_i ” ($i = \{1, 2, 3\}$) is the region of the resonance energy corresponding to the scattering with the mass eigenstate ν_i of cosmic neutrino background. The vertical lines with $T_\nu(z = \{0, 2\})$ indicate the temperatures of $C\nu B$ at $z = \{0, 2\}$. All the neutrino masses in our reference choices, which are also marked with the vertical lines, are significantly larger than the temperatures; The inclusion of the thermal distribution effect of $C\nu B$ momentum does not change our numerical results.

We have checked numerically the $C\nu B$ momentum effect does not drastically change our conclusions drawn in this section. We will come back to this point at the end of this section.

In the following calculations, we will use the best-fit values of the mixing angles and the mass squared differences from Ref. [92]:

$$\begin{aligned} \sin^2 \theta_{13} &= 0.0234 \text{ (0.0240)}, \quad \sin^2 \theta_{23} = 0.567 \text{ (0.573)}, \\ \sin^2 \theta_{12} &= 0.323, \quad \Delta m_{21}^2 = 7.60 \times 10^{-5} \text{ [eV}^2\text{]}, \\ |\Delta m_{31}^2| &= 2.48 \text{ (2.38)} \times 10^{-3} \text{ [eV}^2\text{]} \end{aligned} \quad (15)$$

for the normal (inverted) mass hierarchy, and the CP violating phase is set to be zero.

A. Reproduction of the gap with the SFR

To begin with, we check if the gap can be reproduced by the resonant $L_\mu - L_\tau$ scatterings. Since neutrino consists of three generations, we generally expect three gaps in the spectrum. In Fig. 2, the resonance energies E_{res} are plotted as functions of the lightest neutrino mass m_{lightest}

with different values of $M_{Z'}$ and with both the mass hierarchies. It can be read off from the plots that in order to reproduce a single gap, the masses of neutrinos should be quasi degenerate so that the three of the resonance energies are located at the same point. In Fig. 3, we show the cosmic neutrino flux with the attenuation effect by the $L_\mu - L_\tau$ force and compare the results with three different values of the spectral index s_ν . Here we take the normal hierarchy with the lightest neutrino mass $m_1 = 0.08 \text{ eV}^4$ and set the model parameters as $M_{Z'} = 11 \text{ MeV}$ and $g_{Z'} = 5 \times 10^{-4}$. For the sources of cosmic neutrinos, we assume the SFR, which is given at Eq. (10), as their redshift distribution, and the cut-off energy E_{cut} , which appears in Eq. (9), is taken as $E_{\text{cut}} = 10^7 \text{ GeV}$. The normalization factor \mathcal{Q}_0 is adjusted so that the magnitude

⁴ This leads to $\sum m_\nu \simeq 0.25 \text{ eV}$, which is slightly higher than the 95% C.L. limit from the combined analysis of cosmological observations [93]. However, once the cosmological model is extended to include more parameters, the constraint is expected to be relaxed. For instance, simultaneous inclusion of N_{eff} and $\sum m_\nu$ leads to $\sum m_\nu < 0.28 \text{ eV}$ [93].

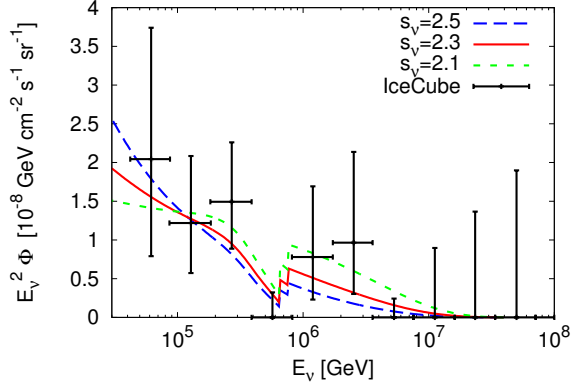


FIG. 3. The cosmic neutrino fluxes calculated with the $L_\mu - L_\tau$ gauge interaction are compared with the three-year IceCube data [3]. The model parameters are taken as $M_{Z'} = 11$ MeV and $g_{Z'} = 5 \times 10^{-4}$. The lightest neutrino mass is set to be $m_1 = 0.08$ eV and the normal mass hierarchy is chosen. The SFR is assumed as the redshift distribution of the cosmic neutrino sources. The cut-off energy of the original flux is placed at $E_{\text{cut}} = 10^7$ GeV. The three different values of the spectral index s_ν are examined.

of the calculated flux fits the observation. As can be seen from the figure, the flux is significantly attenuated round 400 TeV – 1 PeV. With a spectrum including the gap, one can expect a relatively good fit to the observation even with a lower spectral index such as $s_\nu \lesssim 2.2$. Since the spectrum calculated with the inverted hierarchy is essentially the same as the normal hierarchy shown at Fig. 3, we do not repeat it.

B. Source distributions

So far, we have adopted the SFR as the redshift distribution of cosmic neutrino sources in our calculations. However, the source has not been specified yet, and some of the astrophysical objects have been discussed as the candidate [10–15]. In Fig. 4, we examine the distribution of gamma-ray bursts (GRBs) [94]:

$$\mathcal{W}_{\text{GRB}}(z) \propto \begin{cases} (1+z)^{4.8} & 0 \leq z < 1, \\ (1+z)^{1.4} & 1 \leq z \leq 4.5 \end{cases} \quad (16)$$

and the monotonic evolution distribution [95]:

$$\mathcal{W}_{\text{mono}}(z) \propto (1+z)^m \quad (17)$$

with $m = 2$, $z_{\text{max}} = 4$ and $m = 5$, $z_{\text{max}} = 1$, and compare them to the result calculated with the SFR. Here, the spectral index is set to be $s_\nu = 2.3$. The neutrino mass spectrum and the model parameters are taken to be the same as Fig. 3. It is natural to conclude that, if the power-law spectrum Eq. (9) is assumed, the types of source distribution do not make a big impact on a shape of the flux. One can expect to find the difference caused

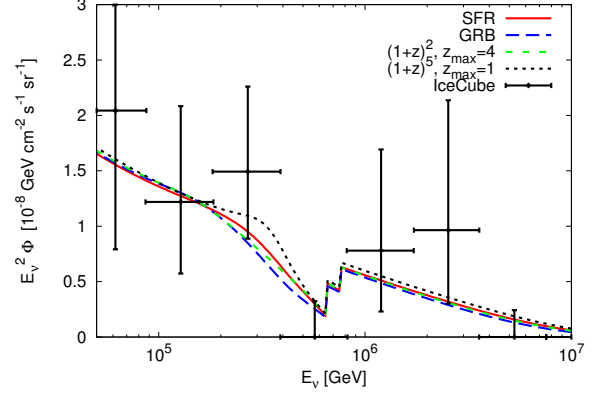


FIG. 4. Same as Fig. 3 with different types of source distributions. The spectral index is taken as $s_\nu = 2.3$.

by the choice of source distribution at the energy region slightly below the resonance point, at which the effect of regeneration is relevant.

C. Simultaneous reproduction of the gap and the edge

Although the best-fit value of the spectral index is evaluated as $s_\nu = 2.5$ from the observation [4–8], it is pointed out in Refs. [9–11] that cosmic neutrino from pp reaction with the spectral index higher than 2.2 predict too high gamma-ray rate at the GeV–TeV range. One of the reasons of such a high best-fit value is the sharp edge in the spectrum at 3–4 PeV. In view of these considerations, we here take lower values of s_ν and attempt to form the edge at the upper end of the spectrum by means of the $L_\mu - L_\tau$ interaction, instead of setting the cut-off energy. Note that with an appropriate adjustment of the flux normalization, lower values of the spectral index can still give a good fit to the current observed spectrum [7, 8]. According to Fig. 2, the mass of the lightest neutrino should be smaller than 10^{-2} eV to split the resonance energies and distribute them to the positions of the gap and the edge. The mass of Z' should be smaller than $M_{Z'} \lesssim 20$ MeV to place the resonance energies at the appropriate positions, cf. Eq. (2). In Fig. 5 (6), we set the mass of Z' to 9 MeV, the coupling $g_{Z'}$ to 4×10^{-4} , and the lightest neutrino mass m_1 (m_3) to 6×10^{-3} eV with the normal (inverted) hierarchy of neutrino masses. Here, the SFR is assumed as the source distribution $\mathcal{W}(z)$, and the cut-off energy is taken to be sufficiently high so that the numerical results do not depend on the value. The gap is successfully reproduced by the scattering with the heaviest mass eigenstate of $C\nu B$. On the other hand, the resonant scattering for the edge might be insufficient: the flux is attenuated only between 3–7 PeV, which might be too narrow (and also too shallow) to reproduce the expected property of the edge, although it is consistent with the current data. Lastly, let us comment on the

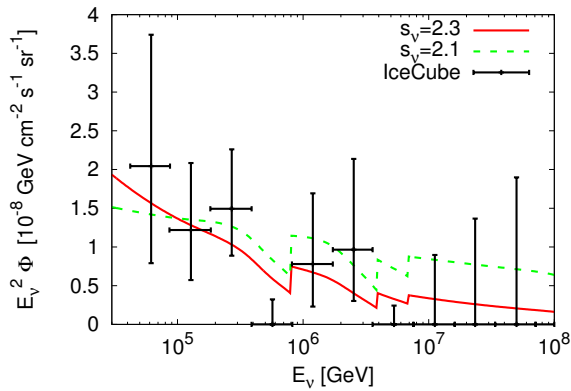


FIG. 5. The cosmic neutrino flux calculated with $M_{Z'} = 9$ MeV and $g_{Z'} = 4 \times 10^{-4}$. Here the normal hierarchy is chosen and the lightest neutrino mass is set to be $m_1 = 6 \times 10^{-3}$ eV. The spectral index is taken to be $s_\nu = 2.3$ and 2.1.

effect of the $C\nu B$ momentum. If the lightest neutrino mass is chosen to be as light as the $C\nu B$ temperature, the $C\nu B$ momentum effect is expected to become appreciable, which would make the width of the edge wider. We will study this possibility in near future.

V. DISCUSSION AND CONCLUSIONS

We have introduced an anomaly-free leptonic force mediated by the gauge boson with a mass of the MeV scale in order to explain simultaneously the two phenomena with different energy scales in lepton physics: (i) the disagreement between experimental measurement and theoretical predictions in muon anomalous magnetic moment, and (ii) the characteristic features of the cosmic neutrino spectrum reported by the IceCube collaboration. Assuming that the PeV cosmic neutrinos are produced after the pp inelastic scattering process in cosmic-ray reservoirs, we have calculated diffuse neutrino flux with the new leptonic force.

We have discussed the relevant constraints, such as the lepton trident process and the observation of solar neutrino event at the Borexino, and scanned the model parameter space. We have found the choices of parameters, which successfully reproduce the measured value of muon anomalous magnetic moment and the gap between 400 TeV and 1 PeV in the IceCube spectrum.

Setting the mass of the leptonic gauge boson to be around 10 MeV and the lightest neutrino mass to be lighter than $\mathcal{O}(10^{-2})$ eV, we could arrange the three resonant energies E_{res} corresponding to three mass eigenstates of cosmic neutrino background to the energy ranges of the gap ($E_\nu = 400$ TeV-1 PeV) and the edge ($E_\nu \simeq 3$ PeV) simultaneously. However, the resonance at the energy corresponding to the edge might be too narrow (and too shallow) to explain the sharp upper end of the spectrum, which is expected from the observation of

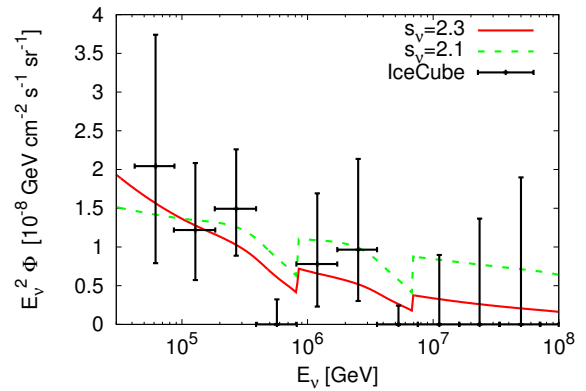


FIG. 6. Same as Fig. 5 with the inverted mass hierarchy.

the IceCube. If one considers the parameter region where the lightest neutrino mass is much lighter than $\mathcal{O}(10^{-2})$ eV, momentum distribution of $C\nu B$ begins to have an impact, and one can expect that the inclusion of the effect would make the resonant region wider. We are now preparing for our next analysis in which we will examine the thermal effect of $C\nu B$ with smaller neutrino masses.

We have also examined the different redshift distribution of cosmic neutrino sources and compared the resulted spectra with each other, assuming the power-law spectrum for the original flux. One can expect the visible difference in the spectrum just below the energy region of the gap.

Before closing this paper, we make some comments on Ref. [46] which has some overlap with our study. In Ref. [46], the authors also considered the $L_\mu - L_\tau$ model and discussed its impact on the cosmic neutrino spectrum as well as muon anomalous magnetic moment. One of the main conclusions of Ref. [46] is that the leptonic force with $M_{Z'} \simeq 1$ MeV significantly reduces the cosmic neutrino flux in a wide energy range between $E_\nu = \mathcal{O}(100)$ TeV and $\mathcal{O}(1)$ PeV with the lightest neutrino lighter than 10^{-3} eV. In contrast, we have set $M_{Z'} \simeq 10$ MeV and $m_{\text{lightest}} \gtrsim 10^{-3}$ eV, and also paid a special attention to the gap and the upper edge in the spectrum. Therefore, our study is complementary with Ref. [46] in the sense of the model parameter region and a viewpoint. Furthermore, we have discussed the experimental bounds to the leptonic force and included the constraints from the loop-induced ν - e scattering process [73] and the BBN [45], both of which disfavour the possibility of the Z' as light as $\mathcal{O}(1)$ MeV. We have confirmed that our numerical method correctly reproduced the results of Ref. [46] in the parameter region with $m_{\text{lightest}} \gtrsim 10^{-2}$ eV.

ACKNOWLEDGMENTS

We gratefully acknowledge insightful comments of Prof. Shigeru Yoshida. We thank Prof. Masahiro Ibe and Dr. Ayuki Kamada for valuable comments on con-

straints to the model, Prof. Kazunori Kohri for pointing out importance of the relation between cosmic neutrino and gamma-ray observations, and Dr. Irene Tamborra for helpful comments on cosmic neutrino propagation. T.O. is grateful to the Mainz Institute for Theoretical Physics (MITP) for its hospitality and support and would like to express a special thanks to the organisers and the participants of *Crossroads of neutrino physics* for many constructive comments, particularly,

Prof. André de Gouvêa and Prof. Joachim Kopp for useful comments on the constraints to the leptonic interactions, Prof. Zurab Berezhiani and Dr. Claudia Hagedorn for discussion on the symmetry and its breaking, and Prof. Pasquale Serpico for his helpful and encouraging comments and suggestions. This work is supported by JSPS KAKENHI No. 26105503 (T.O.), No. 24340044, No. 25105009 (J.S.), and No. 15K17654 (T.S.).

-
- [1] M. Aartsen *et al.* (IceCube Collaboration), Phys.Rev.Lett. **111**, 021103 (2013), 1304.5356.
 - [2] M. Aartsen *et al.* (IceCube), Science **342**, 1242856 (2013), 1311.5238.
 - [3] M. Aartsen *et al.* (IceCube Collaboration), Phys.Rev.Lett. **113**, 101101 (2014), 1405.5303.
 - [4] M. Aartsen *et al.* (IceCube), Phys.Rev. **D91**(2), 022001 (2015), 1410.1749.
 - [5] M. Aartsen *et al.* (IceCube), Phys.Rev.Lett. **114**(17), 171102 (2015), 1502.03376.
 - [6] M. G. Aartsen *et al.* (IceCube) (2015), 1507.03991.
 - [7] S. Palomares-Ruiz, A. C. Vincent, and O. Mena, Phys.Rev. **D91**(10), 103008 (2015), 1502.02649.
 - [8] C. S. Fong, H. Minakata, B. Panes, and R. Zukanovich Funchal, JHEP **1502**, 189 (2015), 1411.5318.
 - [9] A. Loeb and E. Waxman, JCAP **0605**, 003 (2006), astro-ph/0601695.
 - [10] K. Murase, M. Ahlers, and B. C. Lacki, Phys.Rev. **D88**(12), 121301 (2013), 1306.3417.
 - [11] I. Tamborra, S. Ando, and K. Murase, JCAP **1409**(09), 043 (2014), 1404.1189.
 - [12] H.-N. He, T. Wang, Y.-Z. Fan, S.-M. Liu, and D.-M. Wei, Phys. Rev. **D87**(6), 063011 (2013), 1303.1253.
 - [13] R.-Y. Liu, X.-Y. Wang, S. Inoue, R. Crocker, and F. Aharonian, Phys. Rev. **D89**(8), 083004 (2014), 1310.1263.
 - [14] S. Dado and A. Dar, Phys. Rev. Lett. **113**(19), 191102 (2014), 1405.5487.
 - [15] S. Chakraborty and I. Izaguirre, Phys. Lett. **B745**, 35 (2015), 1501.02615.
 - [16] K. Murase (2014), 1410.3680.
 - [17] B. Feldstein, A. Kusenko, S. Matsumoto, and T. T. Yanagida, Phys.Rev. **D88**(1), 015004 (2013), 1303.7320.
 - [18] A. Esmaili and P. D. Serpico, JCAP **1311**, 054 (2013), 1308.1105.
 - [19] A. Ibarra, D. Tran, and C. Weniger, Int.J.Mod.Phys. **A28**, 1330040 (2013), 1307.6434.
 - [20] Y. Bai, R. Lu, and J. Salvado (2013), 1311.5864.
 - [21] Y. Ema, R. Jinno, and T. Moroi, Phys. Lett. **B733**, 120 (2014), 1312.3501.
 - [22] A. Bhattacharya, M. H. Reno, and I. Sarcevic, JHEP **06**, 110 (2014), 1403.1862.
 - [23] J. Zavala, Phys. Rev. **D89**(12), 123516 (2014), 1404.2932.
 - [24] T. Higaki, R. Kitano, and R. Sato, JHEP **07**, 044 (2014), 1405.0013.
 - [25] A. Bhattacharya, R. Gandhi, and A. Gupta, JCAP **1503**(03), 027 (2015), 1407.3280.
 - [26] Y. Ema, R. Jinno, and T. Moroi, JHEP **10**, 150 (2014), 1408.1745.
 - [27] C. Rott, K. Kohri, and S. C. Park, Phys. Rev. **D92**(2), 023529 (2015), 1408.4575.
 - [28] A. Esmaili, S. K. Kang, and P. D. Serpico, JCAP **1412**(12), 054 (2014), 1410.5979.
 - [29] J. Kopp, J. Liu, and X.-P. Wang, JHEP **04**, 105 (2015), 1503.02669.
 - [30] K. Murase, R. Laha, S. Ando, and M. Ahlers (2015), 1503.04663.
 - [31] M. Ahlers, Y. Bai, V. Barger, and R. Lu (2015), 1505.03156.
 - [32] A. Esmaili and P. D. Serpico (2015), 1505.06486.
 - [33] C. E. Aisati, M. Gustafsson, and T. Hambye (2015), 1506.02657.
 - [34] S. B. Roland, B. Shakya, and J. D. Wells (2015), 1506.08195.
 - [35] L. A. Anchordoqui, V. Barger, H. Goldberg, X. Huang, D. Marfatia, L. H. M. da Silva, and T. J. Weiler (2015), 1506.08788.
 - [36] Z. Berezhiani (2015), 1506.09040.
 - [37] S. M. Boucenna, M. Chianese, G. Mangano, G. Miele, S. Morisi, O. Pisanti, and E. Vitagliano (2015), 1507.01000.
 - [38] P. Ko and Y. Tang (2015), 1508.02500.
 - [39] K. Ioka and K. Murase, PTEP **2014**(6), 061E01 (2014), 1404.2279.
 - [40] K. C. Y. Ng and J. F. Beacom, Phys.Rev. **D90**, 065035 (2014), 1404.2288.
 - [41] M. Ibe and K. Kaneta, Phys.Rev. **D90**, 053011 (2014), 1407.2848.
 - [42] K. Blum, A. Hook, and K. Murase (2014), 1408.3799.
 - [43] T. Araki, F. Kaneko, Y. Konishi, T. Ota, J. Sato, *et al.*, Phys.Rev. **D91**(3), 037301 (2015), 1409.4180.
 - [44] J. F. Cherry, A. Friedland, and I. M. Shoemaker (2014), 1411.1071.
 - [45] A. Kamada and H.-B. Yu (2015), 1504.00711.
 - [46] A. DiFranzo and D. Hooper (2015), 1507.03015.
 - [47] V. Barger and W.-Y. Keung, Phys. Lett. **B727**, 190 (2013), 1305.6907.
 - [48] B. Dutta, Y. Gao, T. Li, C. Rott, and L. E. Strigari, Phys. Rev. **D91**, 125015 (2015), 1505.00028.
 - [49] M. S. Bilenky and A. Santamaria (1999), hep-ph/9908272.
 - [50] J. H. Davis and J. Silk (2015), 1505.01843.
 - [51] R. Foot, Mod.Phys.Lett. **A6**, 527 (1991).
 - [52] X. He, G. C. Joshi, H. Lew, and R. Volkas, Phys.Rev. **D43**, 22 (1991).
 - [53] R. Foot, X. G. He, H. Lew, and R. R. Volkas, Phys. Rev. **D50**, 4571 (1994), hep-ph/9401250.
 - [54] S. Choubey and W. Rodejohann, Eur.Phys.J. **C40**, 259 (2005), hep-ph/0411190.

- [55] T. Ota and W. Rodejohann, Phys.Lett. **B639**, 322 (2006), hep-ph/0605231.
- [56] J. Heeck and W. Rodejohann, J.Phys. **G38**, 085005 (2011), 1007.2655.
- [57] J. Heeck and W. Rodejohann, Phys.Rev. **D84**, 075007 (2011), 1107.5238.
- [58] K. Harigaya, T. Igari, M. M. Nojiri, M. Takeuchi, and K. Tobe, JHEP **1403**, 105 (2014), 1311.0870.
- [59] W. Altmannshofer, S. Gori, M. Pospelov, and I. Yavin, Phys. Rev. **D89**, 095033 (2014), 1403.1269.
- [60] J. Kile, A. Kobach, and A. Soni, Phys. Lett. **B744**, 330 (2015), 1411.1407.
- [61] J. Heeck, M. Holthausen, W. Rodejohann, and Y. Shimizu, Nucl. Phys. **B896**, 281 (2015), 1412.3671.
- [62] A. Crivellin, G. D'Ambrosio, and J. Heeck, Phys.Rev.Lett. **114**, 151801 (2015), 1501.00993.
- [63] G. Bennett *et al.* (Muon g-2), Phys.Rev. **D73**, 072003 (2006), hep-ex/0602035.
- [64] M. Davier, A. Hoecker, B. Malaescu, and Z. Zhang, Eur. Phys. J. **C71**, 1515 (2011), [Erratum: Eur. Phys. J.C72,1874(2012)], 1010.4180.
- [65] K. Hagiwara, R. Liao, A. D. Martin, D. Nomura, and T. Teubner, J.Phys. **G38**, 085003 (2011), 1105.3149.
- [66] T. Aoyama, M. Hayakawa, T. Kinoshita, and M. Nio, Phys. Rev. Lett. **109**, 111808 (2012), 1205.5370.
- [67] A. Kurz, T. Liu, P. Marquard, and M. Steinhauser, Phys. Lett. **B734**, 144 (2014), 1403.6400.
- [68] A. Czarnecki and W. J. Marciano, Phys. Rev. **D64**, 013014 (2001), hep-ph/0102122.
- [69] S. Baek, N. Deshpande, X. He, and P. Ko, Phys.Rev. **D64**, 055006 (2001), hep-ph/0104141.
- [70] D. Geiregat *et al.* (CHARM-II), Phys. Lett. **B245**, 271 (1990).
- [71] S. Mishra *et al.* (CCFR Collaboration), Phys.Rev.Lett. **66**, 3117 (1991).
- [72] W. Altmannshofer, S. Gori, M. Pospelov, and I. Yavin, Phys.Rev.Lett. **113**, 091801 (2014), 1406.2332.
- [73] R. Harnik, J. Koppe, and P. A. Machado, JCAP **1207**, 026 (2012), 1202.6073.
- [74] S. K. Agarwalla, F. Lombardi, and T. Takeuchi, JHEP **12**, 079 (2012), 1207.3492.
- [75] S. Bilmis, I. Turan, T. M. Aliev, M. Deniz, L. Singh, and H. T. Wong (2015), 1502.07763.
- [76] H. Nunokawa, S. J. Parke, and R. Zukanovich Funchal, Phys.Rev. **D74**, 013006 (2006), hep-ph/0601198.
- [77] L. B. Auerbach *et al.* (LSND), Phys. Rev. **D63**, 112001 (2001), hep-ex/0101039.
- [78] J. D. Bjorken, S. Ecklund, W. R. Nelson, A. Abashian, C. Church, B. Lu, L. W. Mo, T. A. Nunamaker, and P. Rassmann, Phys. Rev. **D38**, 3375 (1988).
- [79] J. D. Bjorken, R. Essig, P. Schuster, and N. Toro, Phys. Rev. **D80**, 075018 (2009), 0906.0580.
- [80] B. Aubert *et al.* (BaBar) (2008), URL <http://www-public.slac.stanford.edu/sciDoc/docMeta.aspx?slac0808.0017>.
- [81] R. Essig, J. Mardon, M. Papucci, T. Volansky, and Y.-M. Zhong, JHEP **11**, 167 (2013), 1309.5084.
- [82] B. Ahlgren, T. Ohlsson, and S. Zhou, Phys. Rev. Lett. **111**(19), 199001 (2013), 1309.0991.
- [83] R. Laha, B. Dasgupta, and J. F. Beacom, Phys.Rev. **D89**(9), 093025 (2014), 1304.3460.
- [84] A. Lessa and O. Peres, Phys.Rev. **D75**, 094001 (2007), hep-ph/0701068.
- [85] F.-Y. Cyr-Racine and K. Sigurdson, Phys.Rev. **D90**(12), 123533 (2014), 1306.1536.
- [86] M. Archidiacono and S. Hannestad, JCAP **1407**, 046 (2014), 1311.3873.
- [87] S. N. Gninenko, N. V. Krasnikov, and V. A. Matveev, Phys. Rev. **D91**, 095015 (2015), 1412.1400.
- [88] Y. Farzan and A. Y. Smirnov, Nucl.Phys. **B805**, 356 (2008), 0803.0495.
- [89] A. M. Hillas, Ann. Rev. Astron. Astrophys. **22**, 425 (1984).
- [90] H. Yuksel, M. D. Kistler, J. F. . Beacom, and A. M. Hopkins, Astrophys.J. **683**, L5 (2008), 0804.4008.
- [91] H. Versteeg and W. Malalasekera, An Introduction to Computational Fluid Dynamics, 2nd edition, Prentice Hall (2007).
- [92] D. Forero, M. Tortola, and J. Valle (2014), 1405.7540.
- [93] P. Ade *et al.* (Planck Collaboration), Astron.Astrophys. (2014), 1303.5076.
- [94] H. Yuksel and M. D. Kistler, Phys. Rev. **D75**, 083004 (2007), astro-ph/0610481.
- [95] S. Yoshida and A. Ishihara, Phys.Rev. **D85**, 063002 (2012), 1202.3522.